OPTICAL PROPERTIES OF MARTIAN DUNITE NWA 2737: A RECORD OF MARTIAN PROCESSES.
C.M. Pieters[1], M.D. Dyar[2], T. Hiroi[1], M.D. Lane[3], A.H. Treiman[4], M. McCanta[4], J.L. Bishop[5], J. Sunshine[6], [1]Dept. Geological Sciences, Brown University, Providence, RI 02912, [Carle_Pieters@brown.edu], [2]Dept. Astronomy, Mount Holyoke College, South Hadley, MA. [3]Planetary Science Institute, Tucson, AZ, [4]Lunar & Planetary Institute, Houston TX, [5] SETI Institute / NASA-Ames Research Center, Mountain View, CA, [6]SAIC, Chantilly, VA.

We have analyzed a subsample of the Martian olivine meteorite NWA2737 as a consortium in which several analytical techniques were applied to the same samples in sequence. Detailed petrology and chemistry (including ferric/ferrous assessment) is reported in a companion abstract [1]. We summarize here spectroscopic measurements made at visible, near-infrared and min-infrared wavelengths. These are compared to other Martian and terrestrial samples for assessment of the features observed.

NWA2737 is an unusual meteorite. As the second Martian dunite, it can be compared directly to Chassigny and is found to exhibit slightly more Mg-rich minerals [2,3]. In evaluation of its petrology, however, it is clear this meteorite has experienced a very different history. All authors have commented on the "brown" appearance of the olivine. As discussed below, there are several mechanisms that will cause olivine to appear "brown". Other Martian olivines (e.g. ALHA77005) have been described with similar but less pervasive characteristics, and the most quoted cause for the "brown" color in the literature is in associated with shock [4], and specifically shock in an oxidizing environment [5].

Spectroscopic measurements. Shown in Figures 1, 2, and 3 are visible to mid-infrared spectra of the same NWA2737 whole rock and olivine separates. All but one (chip in Fig 3b) are measured as particulate separates, either <45 μm or 45-125 μm. Data were measured as reflectance in the RELAB using the bidirectional spectrometer (Fig 1) or Nicolet-Pike off-axis biconical spectrometer (Figs 2, 3a) [6]. Emissivity data [Fig. 3b] were measured at Arizona State Univ. [7].

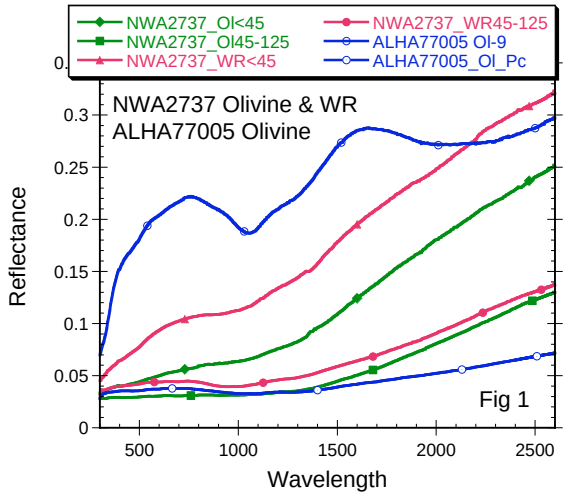

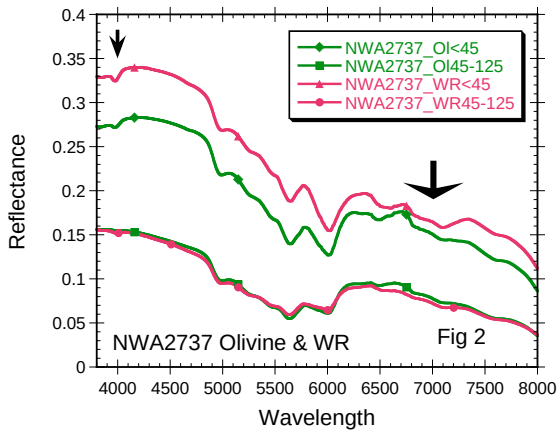

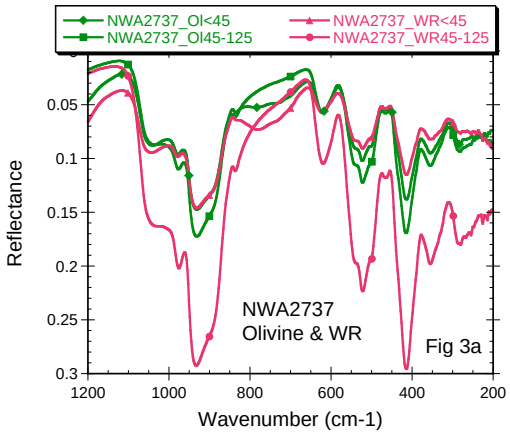

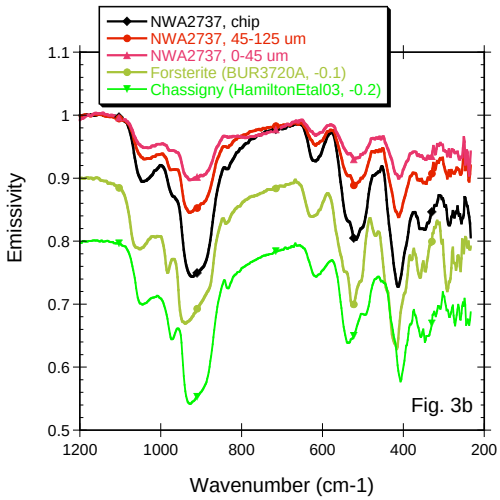

Figures 1, 2, 3. Reflectance and Emission spectra of NWA2737 olivine (dark green) and whole rock (red) size separates. A few additional Martian meteorites are shown for comparison. In Fig 2 arrows indicate carbonate absorptions; all others are olivine. Colors and symbols for each NWA2737 size separate are the same for all figures.

Visible to near-infrared [Fig 1]. Without additional data, it would be difficult, if not impossible, to interpret these spectra. Both the whole rock and the olivine separates exhibit the same unusual optical properties: monotonically increasing reflectance with a broad feature extending beyond 1 µm. The three expected crystal-field [CF] absorptions due to olivine are barely detectible, if at all. For comparison, spectra for two different olivine separates of ALHA77005 are shown. Only the brighter separate exhibits prominent CF bands of olivine.

Extended near-infrared [Fig 2]. Well developed overtones of olivine vibrational bands in the mid-infrared are easily identified between 5–6 µm. Trace amounts of carbonate seen in thin section [1] are also detected based on diagnostic features at 4 and 7 µm. This part of the spectrum appears unaffected by whatever suppresses features at shorter wavelengths.

Mid-infrared [Fig. 3]. Essentially all the observed vibrational features can be attributed to fosterite olivine. From these spectra alone, there is no question that the samples are composed of crystalline mg-olivine. There is nothing to suspect anything unusual about these samples. A few other features are notable. The small volume scattering behavior present in the <45-µm fractions between 800-650 cm-1 results in a weak "transparency feature" [8]. A possible cause for a weaker ~980 cm^{-1} feature observed in the chip emissivity spectrum (Fig 3b) could be that the olivines have a preferred orientation in the rock chip measured.

Discussion. The near-infrared and mid-infrared spectra tell two entirely different stories about this olivine Martian meteorite. On the one hand, from the mid-infrared it is clear that the molecular structure and composition of the olivine is well defined and is not significantly different from other well characterized mg-olivines. On the other hand, the visible to near-infrared spectra indicate that some process has pervasively altered the nature of characteristic electronic transitions of iron in the olivine M1 and M2 sites. The origin of the "brown" olivine of this meteorite and the cause of its unusual visible to near-infrared properties need to be understood. If this property is found to be common, it provides an additional tool to interpret remote analyses of the Martian surface and constrain surface processes.

Additional clues. As described in [1] there appears to be a preferred association of both the "brown" and the visibly colorless (vc) olivine of NWA2737 along deformation slip planes. The "brown" olivine is also brighter in BSE images, implying a slightly greater density. Unlike the vc olivine, the "brown" olivine has few of the types of fractures linked to shock events, consistent with shock annealing described by [5].

Possible causes of "brown" olivine. Unaltered fosterite is relatively transparent at visible wavelengths (400-700 nm) and appears visually colorless in thin section (vc in [1]). Olivine appears "green" in hand specimen because the reflectance of olivine peaks in the part of the spectrum most sensitive to the human eye, where solar radiation also peaks, between 550-600 nm. Any deviation to this results in "colored" olivine to the human eye in petrographic analyses.

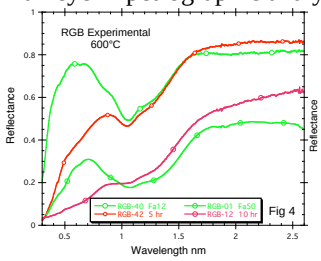

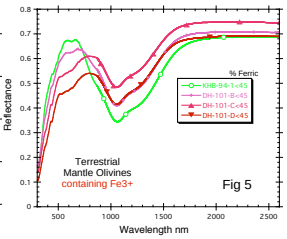

There are several very different causes for "brown" or "colored" olivine, illustrated in Fig 4&5. Processes that produce olivine of a different color at visible wavelengths include: 1) *Terrestrial-type weathering*. Olivine is transformed into iddingsite or other ferric-bearing phases. The visible color is dominated by ferric absorptions. 2) *Thermal metamorphism in an oxidizing environment.* Burns [9] reproduced this experimentally (Fig 4) and suggested both structural Fe^{3+} and ferric phases are the cause of observed absorptions. He also produced examples of low temperature olivine oxidation in acidic brines with ferric sulfate. 3) *Rapid melting and recrystalization* (with abundant microcrystals). This involves phase transitions, but a color may be due to scattering of dispersed nanophase components. 4) *Subsolidus homogeneous oxidation* (+annealing) *from shock at high* pO_2. This is observed experimentally [5]; at low pO_2 annealing occurs without oxidation. 5) *Dehydration during assent from H-bearing source*. This can produce ferric bearing olivine [10,1], but may not exhibit strong visible color (Fig 5). 6) *Olivine composition.* Iron-rich olivines are generally much darker than their magnesium-rich cousins. In thin section the iron-rich form appears browner. All but #3 and 6 imply the presence of Fe^{3+} and absorptions due to metal-metal or oxygen-metal electronic transitions that extend into the near-infrared.

Conclusions. The above options for "brown" olivine are not all mutually exclusive. Given the compositional and petrographic data for NWA2737, processes involved in #4 and/or a combination of #3+5 appear the most viable to be rigorously tested.

References. 1.Trieman et al. 2006, these volumes. 2. Beck et al. 2005, LPSXXXVI #1326; 2006, *GCA* 70, in press. 3. Mikouchi et al. 2005, LPSXXXVI #1944. 4.Ostertag et al., 1984, E*PSL*, *67*, 162. 5. Bauer, 1979, *Proc. Lunar Planet. Sci. Conf., X*, 2573. 6. Pieters and Hiroi, 2004 LPSXXXV #1720. 7. Ruff et al., 1997, JGR 102, 14899. 8. Salisbury, J. and Walter, L., 1989, *JGR*, *94*, 9192. 9. Bartels and Burns 1989 LPSXX, 44; Fisher and Burns LPSXX, 299; Burns LPSXX 129. 10. Dyar M.D. 2003, *MaPS 38*, 1733,

Acknowledgments. RELAB is a multiuser facility operated under NASA grant NAG5-13609. This research is supported by NASA grants NNG04GB53G, NNG04GG12G, and NAG5-12687, NAG5-12271 and NAG5-13279.